

Mesoscale Meteorology: Frontal Analysis and Frontogenesis

21, 23 February 2017

What is a Front?

A front represents a transition zone between contrasting air masses, with mesoscale horizontal density and temperature gradient magnitudes that are much larger than their synoptic-scale values. The cross-front scale [$O(100\text{ km})$] is decidedly mesoscale, whereas the along-front scale [$O(1000\text{ km})$] is decidedly synoptic-scale. Fronts are thus an elongated zone of locally-large horizontal temperature gradient: $\sim 10\text{ K}/100\text{ km}$ versus typical synoptic-scale values of $\sim 10\text{ K}/1000\text{ km}$. They represent horizontal temperature gradient discontinuities: positive ahead to negative behind a front. The region of locally-enhanced horizontal temperature gradient magnitude is sometimes referred to as a *baroclinic zone*.

Due to the thermal wind relationship, fronts are regions of locally-enhanced vertical wind shear. This is manifest through a symbiotic relationship between fronts and jets. Consequently, fronts are also zones where available potential energy is maximized. Further, cyclonic horizontal wind shear is maximized across fronts, so that cyclonic vertical vorticity is maximized and sea-level pressure and geopotential height are minimized along fronts. Fronts are typically located ahead of synoptic-scale upper-tropospheric troughs in regions of synoptic-scale forcing for ascent.

For air parcels originating at the altitude of a given front, static stability is maximized behind cold fronts and ahead of warm fronts. This manifests as a frontal inversion on soundings released from within a frontal zone. Thus, while fronts serve as foci for rising motion, clouds, and precipitation, there are preferred locations for where these features are found with respect to frontal zones, as we will demonstrate shortly for both cold and warm fronts.

Fronts can be located anywhere within the troposphere. The strongest fronts extend upward from the surface to the tropopause; however, many fronts are shallower in nature and are located either in the lower troposphere or the middle to upper troposphere. While upper tropospheric fronts and their accompanying tropopause folds are important for post-frontal mesoscale precipitation bands, particularly in maritime locations, our focus in this class is on fronts that are strongest at and near the surface; these are known as *surface* fronts.

There are four primary frontal classifications: cold, warm, stationary, and occluded. In the interest of brevity, we will not consider occluded fronts in this class. Stationary fronts are considered only briefly. Fronts need not remain of a single classification; in fact, many fronts “originate” as cold fronts trailing surface cyclones, become stationary after advancing equatorward, and finally retreat poleward as warm fronts in advance of a new surface cyclone. For illustrative purposes, however, it is convenient to first consider each in isolation.

Cold Fronts

When a relatively cold air mass advances toward a relatively warm air mass, the boundary separating the two air masses is known as a cold front. Cold fronts are located along the leading edge of the cold air; the cold frontal zone extends rearward from the cold front to where

temperature ceases to drop rapidly (i.e., where the horizontal temperature gradient magnitude diminishes to its synoptic-scale value). Ahead of cold fronts, winds veer with height, signifying warm air advection; behind cold fronts, winds back with height, signifying cold air advection.

Cold fronts slope rearward over the cold air mass; i.e., they slope upward in the rearward direction. The typical vertical slope of a cold frontal zone is on the order of 1 km upward for every 100 km of horizontal distance. It has steepest slope near the surface and smaller slope at higher altitudes. Cold frontal zones have a vertical depth of 500-1500 m. Within this zone, potential temperature increases rapidly with height; thus, cold frontal zones are regions of elevated static stability. Deep turbulent vertical mixing is common behind cold fronts, increasing the slope of the cold air at the front's leading edge and promoting downward momentum transport and gusty surface winds.

Warm Fronts

When a relatively cold air mass retreats in advance of a relatively warm air mass, the boundary separating the two air masses is known as a warm front. Warm fronts are located along the rear edge of the advancing warm air; the warm frontal zone extends forward from the warm front to where the temperature ceases to drop rapidly. Winds veer with height ahead of warm fronts, signifying warm air advection. Depending on the proximity to an advancing cold front, winds in the wake of a warm front may change little or weakly veer with height.

Warm fronts slope forward over the cold air mass; i.e., they slope upward in the forward direction. The typical vertical slope of a warm frontal zone is on the order of 1 km upward for every 200 km of horizontal distance. It has steepest slope near the surface and smaller slope at higher altitudes. Similar to cold fronts, warm frontal zones have a vertical depth of 500-1500 m over which potential temperature rapidly increases with height. However, horizontal and vertical temperature gradients are typically not as strong with warm fronts as with cold fronts.

Stationary Fronts

Fronts that exhibit little or no motion are termed *stationary fronts*. Cold or warm fronts can become stationary fronts when their motion slows, as commonly occurs when the horizontal wind becomes oriented largely parallel to the front itself. With stationary fronts, colder air masses do not advance toward or retreat from warmer air masses. Precipitation associated with stationary fronts is usually of a stratiform, or non-convective, nature. However, stationary fronts are often foci for mesoscale convective system formation and movement during the warm-season. They also serve as the focus along which new synoptic-scale cyclones form and move.

Frontal Motion and Slope

Cold front and warm front motion are governed by the component of wind perpendicular to the front within the cold air. Frontal motion is more rapid when the wind ahead of the front is more perpendicular to the front and in the same direction as its motion. Note that the extent to which the wind is perpendicular to the front can and often does vary along a front. Fronts move toward areas of falling sea-level pressure or height. When sea-level pressure or height falls more rapidly ahead of a front, and thus rises more rapidly behind a front, the front moves more rapidly. Warm front motion is thus often slowest when strong anticyclogenesis is found poleward of the warm front.

Consider the case of frontogenesis, distilled here as “warming where already warm and cooling where already cool.” This is associated with increasing layer thickness on the warm side of a front and decreasing layer thickness on the cold side of a front. This promotes falling sea-level pressure or height at the bottom of the layer on the warm side of a front and rising sea-level pressure or height at the bottom of the layer on the cold side of a front. This establishes an ageostrophic flow from the cold side to the warm side of a front. This ageostrophic flow is perpendicular to the cold front in the direction of its motion and perpendicular to the warm front in the opposite direction of its motion. Consequently, cold fronts typically move more rapidly than warm fronts, particularly in frontogenetic situations.

As noted earlier, cold fronts typically have steeper slope than warm fronts. There are two primary reasons why: surface friction and diabatic heating. Surface friction acts to slow the surface wind; its effects diminish rapidly with height. Friction acts to slow the advance of cold air behind a cold front and the retreat of cold air ahead of a warm front. For a cold front, cold air above the surface is not impacted; thus, it has the appearance of “catching up” to the surface cold front. For a warm front, warm air above the surface is not impacted; thus, it has the appearance of “outrunning” the surface warm front. This results in cold fronts having steeper near-surface slope than warm fronts.

The contribution of diabatic heating to near-surface frontal slope manifests in surface heat fluxes. Ahead of a cold front, the air is relatively warm; this warms the underlying soils. After the cold front passes, the air is relatively cold. In this scenario, sensible heat flux is directed from soil to air (or, more generally, is directed more from soil to air than before front passage). By contrast, ahead of a warm front, the air is relatively cool. After the warm front passes, the air is relatively warm. In this scenario, sensible heat flux is directed from air to soil (or, more generally, is directed more from air to soil than before front passage). The former scenario promotes stronger, deeper vertical mixing, which acts to vertically-homogenize potential temperature over the mixed layer. Along the front’s leading edge, this results in a steeper frontal slope. The latter scenario promotes weaker, shallower vertical mixing, resulting in a shallower frontal slope along the front’s leading edge. This is exacerbated by differences in insolation behind cold fronts versus ahead of warm fronts: stronger insolation is typically found behind cold fronts than ahead of warm fronts, for reasons described in the next subsection.

The steeper slope of cold fronts relative to warm fronts promotes stronger, vertically-deeper ascent along a cold front’s leading edge; i.e., it promotes stronger forcing against stable stratification as manifest by CIN, thus increasing the likelihood that ascending air parcels will become positively buoyant upon ascent. Thus, deep, moist convection is said to be more likely along cold fronts than along and ahead of warm fronts, although the particulars critically depend upon environmental characteristics associated with each feature that vary between events.

Three-Dimensional Frontal Cyclone Structure

Mid-latitude cyclones are characterized by four primary air streams: *primary (W1) and secondary (W2) warm conveyor belts*, a *cold conveyor belt (CCB)*, and a *dry intrusion (DI)*; Fig. 1).

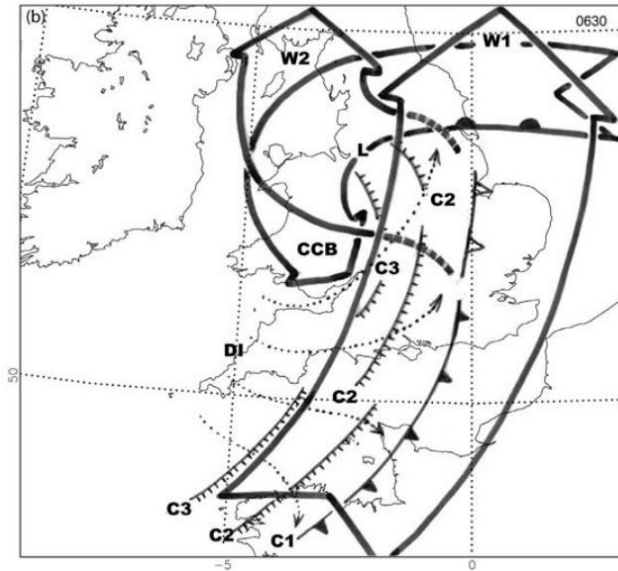


Figure 1. Idealized depiction of the primary air streams of a developing frontal cyclone. Figure reproduced from Browning (2005, *Quart. J. Roy. Meteor. Soc.*), their Fig. 4b.

The primary warm conveyor belt ascends from near the surface within the warm air to the middle and, ultimately, upper troposphere as it ascends over the warm front. It may turn anticyclonically after ascending over the warm frontal zone. Recall that warm fronts slope forward over a cold air mass; i.e., isentropes slope upward over the cold air mass. For flow along an isentrope (e.g., no change in potential temperature following the motion), it must ascend as it approaches a warm front. The primary warm conveyor belt is thus responsible for cloud and precipitation development along and poleward of a warm frontal zone. Stratiform precipitation is favored poleward of warm frontal zones, although released elevated instability can lead to embedded deep, moist convection.

The secondary warm conveyor belt also ascends from near the surface within the warm air to the middle troposphere as it ascends over the warm front. It may turn cyclonically after ascending over the warm frontal zone. Middle-tropospheric ascent over the warm frontal zone associated with this conveyor belt is believed to be responsible for the comma head structure on the northwest side of mid-latitude cyclones; this is also a favored region for banded precipitation resulting from strong frontogenesis and/or the release of elevated instability.

The cold conveyor belt ascends gradually from the lower to the middle troposphere poleward of the surface warm frontal zone. It moves rearward with respect to the surface cyclone. As it reaches the cyclone's northwestern quadrant, it may curve cyclonically around the rear of the cyclone.

Finally, the dry intrusion is a descending air stream located immediately rearward of the cyclone. It originates in the middle to upper troposphere and descends to the lower troposphere in the rear of the surface cold front. Recall that cold fronts close rearward over a cold air mass; i.e., isentropes slope downward approaching the cold front from the rear. For flow along an isentropes, it must descend as it approaches a cold front. Thus, this descending air stream is responsible for the lack of middle to high clouds found in the rear of cold fronts; in the case where descent reaches to the lower troposphere, it is responsible for clear skies and drier conditions found behind cold fronts.

The secondary warm conveyor belt typically ascends beneath the descending dry intrusion. This can result in potential instability, with equivalent potential temperature decreasing with height. As demonstrated in our earlier sounding analysis lecture materials, the forced lifting of such a layer results in its destabilization. Such forcing for layer ascent is often found with strong differential cyclonic vorticity advection in advance of the approaching upper tropospheric trough. If the layer can be sufficiently lifted, narrow bands of post-cold frontal convection may develop. This is most common in maritime environments.

Together, the four conveyor belts help us deduce typical mid-latitude cyclone appearance on radar and satellite imagery:

- A fan or delta-shaped area of primarily low- to middle-tropospheric cloud cover poleward of a surface warm frontal zone.
- A comma-shaped cloud region, extending equatorward primarily along the cyclone's cold front. If sufficient instability – whether surface-based ahead of the cold front or elevated in proximity to the secondary warm conveyor belt – exists and can be released, deep, moist convection may be found within one or both of these regions.
- Clear skies or low, primarily stratiform, clouds in the wake of a surface cold frontal zone. Stratiform clouds are favored when sufficiently high lower tropospheric moisture is trapped beneath the cold frontal inversion; they are also common and can sometimes organize into shallow convective cells when cold post-frontal air warms and moistens as it passes over relatively warm water surfaces (e.g., with lake-effect snows). Such clouds are often aligned with the lower tropospheric wind.
- In cases where post-cold frontal potential instability is realized, narrow convective bands aligned with the middle-to-upper tropospheric flow may be found.

Frontal Analysis Principles

To analyze meteorological observations over meso- to synoptic-scale regions, a technique known as *isoplething* is used. Given the prefix *iso-*, isopleths connect locations on a map of meteorological observations that have equal values of the variable being analyzed. Common isopleths include isotherms, isentropes, isodrotherms, isotachs, isobars, isallobars, and isohyses for temperature, potential temperature, dew point, wind speed, sea-level pressure, sea-level pressure tendency, and geopotential height, respectively.

Isoplething requires interpolating between discrete meteorological observations. Doing so requires the assumption that meteorological fields are continuous, or smoothly- varying. There are several guidelines that should be followed when isoplething:

- Isopleths should satisfy the most applicable conceptual model of the atmosphere.
- Isopleths do not start or stop in the middle of a field; they do not intersect, branch from or merge with one another. They are closed or extend from one edge of the data to another.
- Isopleths only reflect the level of detail allowed by the available data.
- Isopleths are evenly-spaced unless the data or most applicable conceptual model dictate otherwise.

- Isopleths assume that observations are correct unless it can be proven otherwise beyond a reasonable doubt. Observations excluded from an analysis should be circled.
- Isopleths are drawn at appropriate intervals evenly divisible into the isopleth values: e.g., 2 hPa or 4 hPa for isobars, 30 m or 60 m for isohypses, 10 kt or 20 kt for isotachs, and 2-5°C for isotherms, isentropes, and isodrosotherms. Label the ends of all isopleths.

Frontal analysis manifests as application of these principles to frontal structure conceptual models. The following guidelines are used to identify fronts from meso- to synoptic-scale data:

- Start the analysis in a warm air mass and move toward cold air. Where temperature begins to decrease rapidly on the mesoscale provides a first-guess for frontal location. Typically, this results in a front that lies parallel to the isotherms. Repeat for moisture, whether using dew point, mixing ratio, or equivalent potential temperature.
- Identify where isobars or isohypses have greatest kinkiness or cyclonic curvature. Fronts are typically found along the axis of greatest curvature, where sea level pressure or height are minimized.
- Identify where wind direction changes rapidly, with cyclonic curvature, on the mesoscale. Fronts are typically found along the axis of greatest wind direction change.
- Identify where pressure or height tendency changes sign on the mesoscale. Fronts move toward falling sea-level pressure/height and away from rising sea-level pressure/height.
- As frontal motion is fairly consistent through time, extrapolation from frontal analyses at previous times can be used to approximate frontal location at a subsequent analysis time.
- As fronts slope over cold air masses with increasing height, a frontal analysis at one altitude can be used as a first-guess for frontal location at higher and/or lower altitudes.
- The presence, orientation, and type of cloud and precipitation features can be used to refine frontal placement in light of their typical distributions.

Frontogenesis and Frontolysis

A front's intensity is related to the magnitude of the cross-front temperature gradient: stronger fronts have larger cross-frontal temperature gradients. Since potential temperature gradients are equivalent to temperature gradients on isobaric surfaces, we will use temperature gradient to refer to either temperature or potential temperature gradients.

In addition to frontal strength, we are often interested in quantifying how frontal strength changes with time. *Frontogenesis* describes the case where the magnitude of the cross-front temperature gradient increases with time. *Frontolysis* describes the case where the magnitude of the cross-front temperature gradient decreases with time. We quantify frontogenesis and frontolysis in a reference frame moving with the front, or following the motion, such that in two-dimensions we can define frontogenesis as:

$$F = \frac{d}{dt} (\|\nabla_h \theta\|)$$

Here, the subscript of h on the gradient operator explicitly indicates that it is applied on a quasi-horizontal surface, whether height z or pressure p . Formally, frontogenesis is a three-dimensional process, but two dimensions are sufficient to consider its basic characteristics.

Let us first consider the case of a zonally-oriented front, where potential temperature changes only in the north-south direction. For such a front, we are interested in quantifying the change in the magnitude of the meridional potential temperature gradient with time following the motion, i.e.,

$$\frac{d}{dt} \left(- \frac{\partial \theta}{\partial y} \right)$$

The leading negative is for convention only, since temperature generally decreases to the north. We can obtain an expression for this by differentiating the thermodynamic equation with respect to y , i.e.,

$$\frac{\partial}{\partial y} \left(\frac{d\theta}{dt} = \frac{q\theta}{c_p T} \right)$$

First, let us expand the total derivative on the left-hand side of this equation:

$$\frac{\partial}{\partial y} \left(\frac{\partial \theta}{\partial t} + u \frac{\partial \theta}{\partial x} + v \frac{\partial \theta}{\partial y} + w \frac{\partial \theta}{\partial z} = \frac{q\theta}{c_p T} \right)$$

Next, we wish to distribute the partial derivative to each term in this equation:

$$\frac{\partial}{\partial y} \left(\frac{\partial \theta}{\partial t} \right) + \frac{\partial}{\partial y} \left(u \frac{\partial \theta}{\partial x} \right) + \frac{\partial}{\partial y} \left(v \frac{\partial \theta}{\partial y} \right) + \frac{\partial}{\partial y} \left(w \frac{\partial \theta}{\partial z} \right) = \frac{\partial}{\partial y} \left(\frac{q\theta}{c_p T} \right)$$

Apply the product rule to expand the last three terms on the left-hand side of this equation:

$$\frac{\partial}{\partial y} \left(\frac{\partial \theta}{\partial t} \right) + \frac{\partial u}{\partial y} \frac{\partial \theta}{\partial x} + u \frac{\partial}{\partial y} \left(\frac{\partial \theta}{\partial x} \right) + \frac{\partial v}{\partial y} \frac{\partial \theta}{\partial y} + v \frac{\partial}{\partial y} \left(\frac{\partial \theta}{\partial y} \right) + \frac{\partial w}{\partial y} \frac{\partial \theta}{\partial z} + w \frac{\partial}{\partial y} \left(\frac{\partial \theta}{\partial z} \right) = \frac{\partial}{\partial y} \left(\frac{q\theta}{c_p T} \right)$$

We wish to commute the order of partial differentiation on the advection-like terms and group like terms to obtain:

$$\frac{\partial}{\partial t} \left(\frac{\partial \theta}{\partial y} \right) + u \frac{\partial}{\partial x} \left(\frac{\partial \theta}{\partial y} \right) + v \frac{\partial}{\partial y} \left(\frac{\partial \theta}{\partial y} \right) + w \frac{\partial}{\partial z} \left(\frac{\partial \theta}{\partial y} \right) + \frac{\partial u}{\partial y} \frac{\partial \theta}{\partial x} + \frac{\partial v}{\partial y} \frac{\partial \theta}{\partial y} + \frac{\partial w}{\partial y} \frac{\partial \theta}{\partial z} = \frac{\partial}{\partial y} \left(\frac{q\theta}{c_p T} \right)$$

If we group the first four left-hand side terms and move the last three left-hand side terms to the right-hand side of the equation, we obtain:

$$\frac{d}{dt} \left(\frac{\partial \theta}{\partial y} \right) = - \frac{\partial u}{\partial y} \frac{\partial \theta}{\partial x} - \frac{\partial v}{\partial y} \frac{\partial \theta}{\partial y} - \frac{\partial w}{\partial y} \frac{\partial \theta}{\partial z} + \frac{\partial}{\partial y} \left(\frac{q\theta}{c_p T} \right)$$

Or, multiplying by -1,

$$\frac{d}{dt} \left(-\frac{\partial \theta}{\partial y} \right) = \frac{\partial u}{\partial y} \frac{\partial \theta}{\partial x} + \frac{\partial v}{\partial y} \frac{\partial \theta}{\partial y} + \frac{\partial w}{\partial y} \frac{\partial \theta}{\partial z} - \frac{\partial}{\partial y} \left(\frac{q\theta}{c_p T} \right)$$

This equation describes the rate of change in the magnitude of the meridional temperature gradient following the motion. The right-hand side terms represent, from left to right, shearing, diffluence, tilting, and diabatic heating. Positive values of right-hand side forcing terms indicate a larger cross-frontal meridional temperature gradient following the motion; i.e., frontogenesis. We now wish to consider each term in isolation.

Shearing Term

Expressing the frontogenesis equation in terms of only the shearing term, we obtain:

$$\frac{d}{dt} \left(-\frac{\partial \theta}{\partial y} \right) = \frac{\partial u}{\partial y} \frac{\partial \theta}{\partial x}$$

This term is a function of the change in the along-front wind u across the front and the change in potential temperature θ along the front. Note that fronts are typically located parallel to isotherms or isentropes; i.e., in an idealized sense, potential temperature would not change along the front and this forcing term would be zero. However, due to factors such as the meridional variation in insolation, this is often not perfectly true. Thus, this term can be non-zero. An illustrative example is provided in Fig. 2 below.

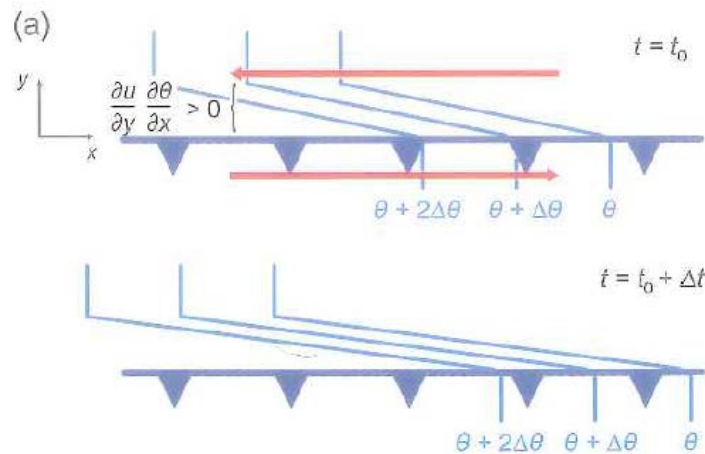


Figure 2. Illustrative example of horizontal shear contributing to frontogenesis. Figure reproduced from Markowski and Richardson (2010), their Fig. 5.4a.

In this example, there is cyclonic horizontal wind shear across the frontal zone. This is as we would expect since fronts are loci of cyclonic vertical vorticity. Differential zonal flow across the frontal zone in this example makes larger the magnitude of the meridional temperature gradient; note the packing of the isentropes north of the front in the top panel versus the bottom panel. However, the difference between panels is not large because the cross-isentrope component of the flow is small.

Diffluence Term

Expressing the frontogenesis equation in terms of only the difflluence term, we obtain:

$$\frac{d}{dt} \left(- \frac{\partial \theta}{\partial y} \right) = \frac{\partial v}{\partial y} \frac{\partial \theta}{\partial y}$$

This term is a function of the change in the cross-front wind v across the front and the change in potential temperature θ across the front. An illustrative example is provided in Fig. 3 below.

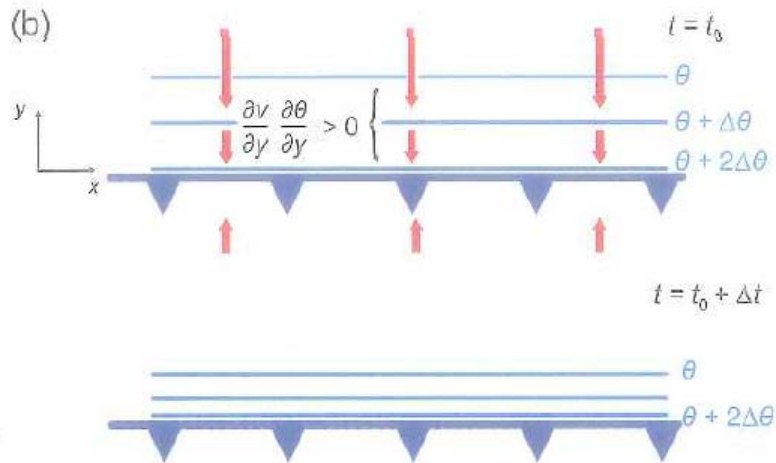


Figure 3. Illustrative example of negative difflluence (confluence) contributing to frontogenesis. Figure reproduced from Markowski and Richardson (2010), their Fig. 5.4b.

In this example, potential temperature decreases along the positive y -axis. However, so does v – it is slightly positive to the south of the frontal zone, slightly negative immediately to the north, and even more negative further to the north. Thus, both partial derivatives in this example are negative, and their product is positive, such that confluence is frontogenetic: it brings isotherms or isentropes closer together. Conversely, it can be shown that difflluence is frontolytic: it spreads isotherms or isentropes further apart.

Tilting Term

Expressing the frontogenesis equation in terms of only the tilting term, we obtain:

$$\frac{d}{dt} \left(- \frac{\partial \theta}{\partial y} \right) = \frac{\partial w}{\partial y} \frac{\partial \theta}{\partial z}$$

This term is a function of the change in vertical velocity w across the front and the vertical variation in potential temperature θ . An illustrative example is provided in Fig. 4 below.

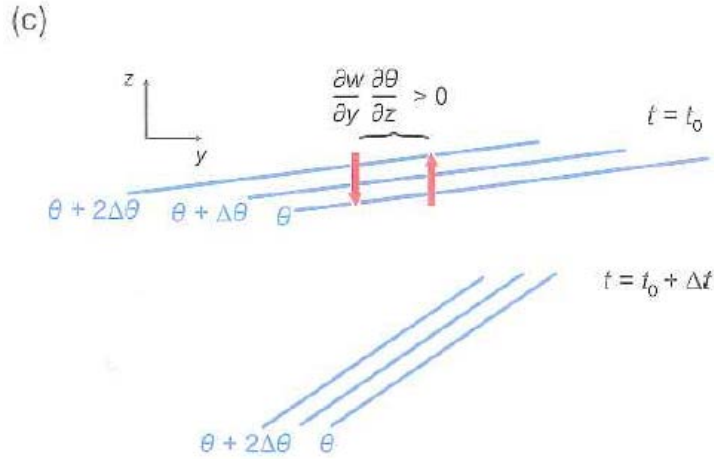


Figure 4. Illustrative example of differential vertical motion across the frontal zone contributing to frontogenesis. Figure reproduced from Markowski and Richardson (2010), their Fig. 5.4c.

In this example, there is ascent on the cold side of the frontal zone and descent along the frontal zone itself. Thus, along the positive y -axis, w becomes more positive – from negative to positive values. Through a frontal inversion, potential temperature rapidly increases with height, such that this term is also positive. Thus, ascent on the cold side of a front and descent on the warm side of a front is frontogenetic. You can view this as “tilting” the isentropes; note the change in slope of these contours between the two panels in Fig. 4 above. The opposite case, with ascent on the warm side of a front and descent on the cold side of a front, is frontolytic.

Diabatic Heating

Expressing the frontogenesis equation in terms of only the diabatic heating term, we obtain:

$$\frac{d}{dt} \left(-\frac{\partial \theta}{\partial y} \right) = -\frac{\partial}{\partial y} \left(\frac{q \theta}{c_p T} \right)$$

This term is a function of the change in diabatic heating rate q across the front. Note that T , c_p , and θ are all positive-definite quantities. When you diabatically warm where it is warm and diabatically cool where it is cool, the front’s strength increases. Conversely, when you diabatically cool where it is warm and diabatically warm where it is cool, the front’s strength decreases. An illustrative example is provided in Fig. 5 below.



Figure 5. Example of meridional variation in diabatic heating contributing to frontogenesis. Figure reproduced from Markowski and Richardson (2010), their Fig. 5.4d.

Here, diabatic cooling, the result of extensive cloud cover blocking insolation from warming the surface, is found north of the frontal zone, with near-zero diabatic heating south of the frontal zone. As a result, diabatic heating becomes more negative along the positive y -axis. The leading negative on this term makes the term positive, defining a frontogenetic situation.

Frontogenesis: Relationship Between Shear and Difffluence

We can develop an analogous equation for the rate of change in the magnitude of the horizontal temperature gradient $\|\nabla_h \theta\| = \sqrt{\left(\frac{\partial \theta}{\partial x}\right)^2 + \left(\frac{\partial \theta}{\partial y}\right)^2}$:

$$\frac{d}{dt} (\|\nabla_h \theta\|) = \frac{d}{dt} \left(\sqrt{\left(\frac{\partial \theta}{\partial x}\right)^2 + \left(\frac{\partial \theta}{\partial y}\right)^2} \right)$$

If we expand the total derivative on the right-hand side of this equation, we obtain:

$$\frac{d}{dt} (\|\nabla_h \theta\|) = \frac{\partial}{\partial t} \left(\sqrt{\left(\frac{\partial \theta}{\partial x}\right)^2 + \left(\frac{\partial \theta}{\partial y}\right)^2} \right) + u \frac{\partial}{\partial x} \left(\sqrt{\left(\frac{\partial \theta}{\partial x}\right)^2 + \left(\frac{\partial \theta}{\partial y}\right)^2} \right) + v \frac{\partial}{\partial y} \left(\sqrt{\left(\frac{\partial \theta}{\partial x}\right)^2 + \left(\frac{\partial \theta}{\partial y}\right)^2} \right)$$

Here, we've neglected the vertical advection term in the definition of the total derivative because we wish to, for now, focus only on the interplay between the shear and difffluence terms. The vertical advection term is not necessary for us to do so, as it only contributes to the tilting term. The equation above is fairly nasty. To help things, we can apply the chain rule, i.e.,

$$\frac{\partial f}{\partial x} \approx \frac{\partial f}{\partial a} \frac{\partial a}{\partial x}$$

where we can let $a = \left(\frac{\partial\theta}{\partial x}\right)^2 + \left(\frac{\partial\theta}{\partial y}\right)^2$. Thus, the above equation can be written as:

$$\frac{d}{dt}(\|\nabla_h\theta\|) = \frac{\partial}{\partial a}\left(a^{\frac{1}{2}}\right)\frac{\partial a}{\partial t} + u\frac{\partial}{\partial a}\left(a^{\frac{1}{2}}\right)\frac{\partial a}{\partial x} + v\frac{\partial}{\partial a}\left(a^{\frac{1}{2}}\right)\frac{\partial a}{\partial y}$$

First find the partial derivative with respect to a :

$$\frac{d}{dt}(\|\nabla_h\theta\|) = \frac{1}{2}a^{-\frac{1}{2}}\frac{\partial a}{\partial t} + u\frac{1}{2}a^{-\frac{1}{2}}\frac{\partial a}{\partial x} + v\frac{1}{2}a^{-\frac{1}{2}}\frac{\partial a}{\partial y}$$

Next, substitute for a and distribute the remaining partial derivatives:

$$\begin{aligned} \frac{d}{dt}(\|\nabla_h\theta\|) = & \frac{1}{2\|\nabla_h\theta\|}\left[\frac{\partial}{\partial t}\left(\left(\frac{\partial\theta}{\partial x}\right)^2\right) + \frac{\partial}{\partial t}\left(\left(\frac{\partial\theta}{\partial y}\right)^2\right)\right] + u\frac{1}{2\|\nabla_h\theta\|}\left[\frac{\partial}{\partial x}\left(\left(\frac{\partial\theta}{\partial x}\right)^2\right) + \frac{\partial}{\partial x}\left(\left(\frac{\partial\theta}{\partial y}\right)^2\right)\right] \\ & + v\frac{1}{2\|\nabla_h\theta\|}\left[\frac{\partial}{\partial y}\left(\left(\frac{\partial\theta}{\partial x}\right)^2\right) + \frac{\partial}{\partial y}\left(\left(\frac{\partial\theta}{\partial y}\right)^2\right)\right] \end{aligned}$$

These terms again benefit from application of the chain rule. This allows us to obtain:

$$\begin{aligned} \frac{d}{dt}(\|\nabla_h\theta\|) = & \frac{1}{2\|\nabla_h\theta\|}\left[2\frac{\partial\theta}{\partial x}\frac{\partial}{\partial t}\left(\frac{\partial\theta}{\partial x}\right) + 2\frac{\partial\theta}{\partial y}\frac{\partial}{\partial t}\left(\frac{\partial\theta}{\partial y}\right)\right] + u\frac{1}{2\|\nabla_h\theta\|}\left[2\frac{\partial\theta}{\partial x}\frac{\partial}{\partial x}\left(\frac{\partial\theta}{\partial x}\right) + 2\frac{\partial\theta}{\partial y}\frac{\partial}{\partial x}\left(\frac{\partial\theta}{\partial y}\right)\right] \\ & + v\frac{1}{2\|\nabla_h\theta\|}\left[2\frac{\partial\theta}{\partial x}\frac{\partial}{\partial y}\left(\frac{\partial\theta}{\partial x}\right) + 2\frac{\partial\theta}{\partial y}\frac{\partial}{\partial y}\left(\frac{\partial\theta}{\partial y}\right)\right] \end{aligned}$$

We can group the terms involving partial derivatives of theta with respect to x ; we can also group the terms involving partial derivatives of theta with respect to y . Each set can be combined into a single total derivative term, such that:

$$\frac{d}{dt}(\|\nabla_h\theta\|) = \frac{1}{\|\nabla_h\theta\|}\left[\frac{\partial\theta}{\partial x}\frac{d_h}{dt}\left(\frac{\partial\theta}{\partial x}\right) + \frac{\partial\theta}{\partial y}\frac{d_h}{dt}\left(\frac{\partial\theta}{\partial y}\right)\right]$$

The subscripts on the total derivatives inside the brackets are intended to clarify that these terms do not contain the vertical advection term.

Earlier, we obtained an expression for $\frac{d}{dt}\left(\frac{\partial\theta}{\partial y}\right)$. An expression for $\frac{d_h}{dt}\left(\frac{\partial\theta}{\partial y}\right)$ is similar, except it neglects the tilting term. If we also neglect the diabatic term, we obtain:

$$\frac{d_h}{dt}\left(\frac{\partial\theta}{\partial y}\right) = -\frac{\partial u}{\partial y}\frac{\partial\theta}{\partial x} - \frac{\partial v}{\partial y}\frac{\partial\theta}{\partial y}$$

In an overarching sense, we are still interested in the tilting and diabatic heating terms. The purpose of this derivation is to clarify the relative roles of the shearing and diffluence terms, however.

An analogous expression for $\frac{d_h}{dt} \left(\frac{\partial \theta}{\partial x} \right)$ takes the form:

$$\frac{d_h}{dt} \left(\frac{\partial \theta}{\partial x} \right) = -\frac{\partial u}{\partial x} \frac{\partial \theta}{\partial x} - \frac{\partial v}{\partial x} \frac{\partial \theta}{\partial y}$$

Substituting these expressions, we obtain:

$$\frac{d}{dt} (\|\nabla_h \theta\|) = \frac{1}{\|\nabla_h \theta\|} \left[\frac{\partial \theta}{\partial x} \left(-\frac{\partial u}{\partial x} \frac{\partial \theta}{\partial x} - \frac{\partial v}{\partial x} \frac{\partial \theta}{\partial y} \right) + \frac{\partial \theta}{\partial y} \left(-\frac{\partial u}{\partial y} \frac{\partial \theta}{\partial x} - \frac{\partial v}{\partial y} \frac{\partial \theta}{\partial y} \right) \right]$$

Or, grouping like terms:

$$\frac{d}{dt} (\|\nabla_h \theta\|) = \frac{1}{\|\nabla_h \theta\|} \left[-\frac{\partial \theta}{\partial x} \frac{\partial \theta}{\partial y} \left(\frac{\partial v}{\partial x} + \frac{\partial u}{\partial y} \right) - \frac{\partial u}{\partial x} \left(\frac{\partial \theta}{\partial x} \right)^2 - \frac{\partial v}{\partial y} \left(\frac{\partial \theta}{\partial y} \right)^2 \right]$$

Recall the definitions of divergence, stretching deformation, and shearing deformation:

$$\delta = \frac{\partial u}{\partial x} + \frac{\partial v}{\partial y} \quad D_{st} = \frac{\partial u}{\partial x} - \frac{\partial v}{\partial y} \quad D_{sh} = \frac{\partial u}{\partial y} + \frac{\partial v}{\partial x}$$

The divergence and stretching deformation form a system of two equations for $\frac{\partial u}{\partial x}$ and $\frac{\partial v}{\partial y}$.

Solving this system for each term, we find:

$$\frac{\partial u}{\partial x} = \frac{1}{2} (\delta + D_{st}) \quad \frac{\partial v}{\partial y} = \frac{1}{2} (\delta - D_{st})$$

Substituting, we obtain:

$$\frac{d}{dt} (\|\nabla_h \theta\|) = \frac{1}{\|\nabla_h \theta\|} \left[-\frac{\partial \theta}{\partial x} \frac{\partial \theta}{\partial y} (D_{sh}) - \frac{1}{2} (\delta + D_{st}) \left(\frac{\partial \theta}{\partial x} \right)^2 - \frac{1}{2} (\delta - D_{st}) \left(\frac{\partial \theta}{\partial y} \right)^2 \right]$$

Group like terms to obtain:

$$\frac{d}{dt} (\|\nabla_h \theta\|) = \frac{1}{\|\nabla_h \theta\|} \left[-\frac{\partial \theta}{\partial x} \frac{\partial \theta}{\partial y} (D_{sh}) - \frac{1}{2} D_{st} \left(\frac{\partial \theta}{\partial x} \right)^2 + \frac{1}{2} D_{st} \left(\frac{\partial \theta}{\partial y} \right)^2 - \frac{1}{2} \delta \left[\left(\frac{\partial \theta}{\partial x} \right)^2 + \left(\frac{\partial \theta}{\partial y} \right)^2 \right] \right]$$

Coordinate geometry can be invoked to show that this can be written as:

$$\frac{d}{dt} (\|\nabla_h \theta\|) = \frac{\|\nabla_h \theta\|}{2} [D_{tot} \cos(2b) - \delta] \quad \text{where } D_{tot} = \sqrt{D_{st}^2 + D_{sh}^2} \text{ (total deformation)}$$

Here, b is the angle between the isentropes and the axis of dilatation, where the *axis of dilatation* is defined as the axis along which the air flow results in the maximum horizontal stretching of air parcels. Contrast this with the *axis of contraction*, which is defined as the axis along which the air flow results in the maximum horizontal contraction of air parcels.

We wish to consider the two terms, total deformation and divergence, in isolation.

Divergence

Considering only the divergence term, we obtain:

$$\frac{d}{dt} (\|\nabla_h \theta\|) = -\frac{\|\nabla_h \theta\|}{2} \delta$$

This term is straightforward to interpret. Here, $\|\nabla_h \theta\|$ is positive-definite. Divergence is where $\delta > 0$, such that the leading negative results in divergence contributing to frontolysis. Conversely, convergence ($\delta < 0$) contributes to frontogenesis. This interpretation is similar, but not quite identical, to that for the diffluence term in the simplified form of this equation. A diffluent wind field has both divergence (in speed) and deformation components. A pure divergent wind field only contains divergence (in speed and direction); there is no deformation. This highlights the key advantage of this formulation, with the deformation part of diffluence subsumed in the shear term.

Total Deformation

Considering only the deformation term, we obtain:

$$\frac{d}{dt} (\|\nabla_h \theta\|) = \frac{\|\nabla_h \theta\|}{2} [D_{tot} \cos(2b)]$$

This term is a bit more complex than the divergence term. It is a function of the angle between the isentropes and the axis of dilatation, which defines the orientation of the isentropes with respect to the deformation wind. For $-45^\circ < b < 45^\circ$, $\cos(2b)$ is positive. For $b < -45^\circ$ or $b > 45^\circ$, $\cos(2b)$ is negative. Thus, when the angle between the isentropes and the axis of dilatation is less than 45° in magnitude, the deformation wind field is frontogenetic; in other words, compression along the axis of contraction dominates relative to stretching along the axis of dilatation. An illustrative example of this is given in Fig. 6a below. Conversely, when the angle between the isentropes and the axis of dilatation is greater than 45° in magnitude, the deformation wind field is frontolytic; in other words, stretching along the axis of dilatation dominates relative to compression along the axis of contraction. An illustrative example of this is given in Fig. 6b. below.

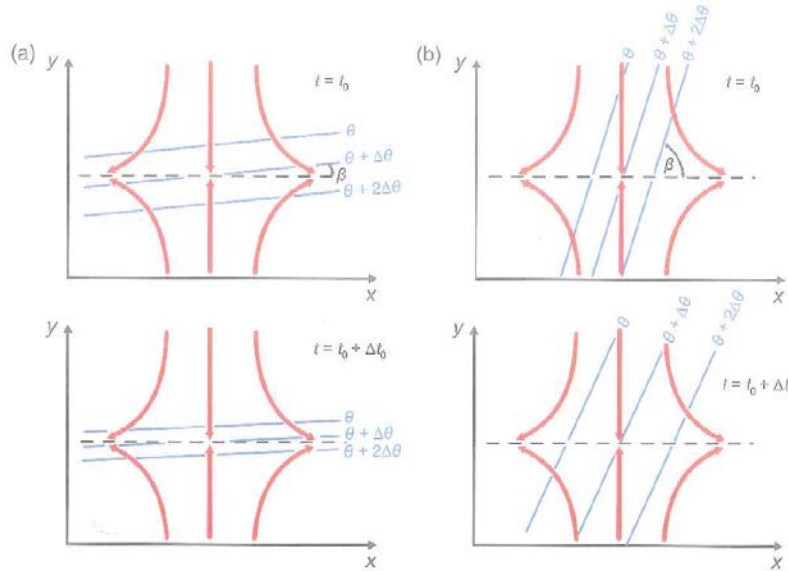


Figure 6. Illustrative examples of (a) deformation leading to frontogenesis and (b) deformation leading to frontolysis as a function of the angle between the isentropes (blue lines) and axis of dilatation (dashed black line). Figure reproduced from Markowski and Richardson (2010), their Fig. 5.5.

What About Vorticity?

Not present in the frontogenesis equation is a vorticity term. Indeed, pure rotation cannot lead to frontogenesis or frontolysis; it can only rotate the isotherms. However, when the flow is not purely rotational, the rotational component of the flow can rotate the isotherms in such a way as to foster a frontogenesis or frontolytic situation. For instance, consider a case where the angle between the isentropes and axis of dilatation is less than 45° (e.g., Fig. 6a). If cyclonic rotation is superimposed on the isentropes, the angle between the isentropes and axis of dilatation will increase, making the otherwise frontogenetical flow less frontogenetical with time.